IOP Publishing | International Atomic Energy Agency Nuclear Fusion

Nucl. Fusion **58** (2018) 126023 (12pp) https://doi.org/10.1088/1741-4326/aae2c5

Simulation of toroidicity-induced Alfven eigenmode excited by energetic ions in HL-2A tokamak plasmas

Hongda He[1], Junyi Cheng[2], J.Q. Dong[1], Wenlu Zhang[2], Chenxi Zhang[2], Jinxia Zhu[3], Ruirui Ma[1], T. Xie[4], G.Z. Hao[1], A.P. Sun[1], G.Y. Zheng[1], W. Chen[1] and Z. Lin[5]

[1] Southwestern Institute of Physics, Chengdu, China
[2] Institute of Physics, Chinese Academy of Science, Beijing, China
[3] School of intelligent manufacturing, Sichuan University of Arts and Science, Dazhou, China
[4] Department of Physics, Sichuan University of Science & Engineering, Zigong 643000, China
[5] Department of Physics and Astronomy, University of California, Irvine, California 92697, United States of America

E-mail: hehda@163.com

Received 21 June 2018, revised 18 September 2018
Accepted for publication 20 September 2018
Published 11 October 2018

Abstract

The toroidicity-induced Alfven eigenmode (TAE) excited by energetic (fast) ions was first simulated using the GTC code for HL-2A experiments. The simulation results indicate that the fraction of energetic ions is about 3% in the experiments. The critical density of energetic ions to excite the TAE mode is around 0.023, which is in good agreement with the theoretical expectation of 0.026. The real frequency of TAE with toroidal mode number $n = 3$ is around 211 kHz and is inversely proportional to the square root of electron density, which is quantitatively in agreement with the experimental observation (Ding *et al* 2013 *Nucl. Fusion* **53** 043015). The frequency is in resonance with the summations of toroidal precession frequency and transit frequency of passing energetic ions, indicating that resonance with passing energetic ions is dominant for the excitation of the modes in the experiment. It is also checked by the phase space structures of $|\delta f_h|^2$ (strength of energetic particle distribution function) that the TAE modes are mainly induced by passing energetic ions in HL-2A. The growth rates of TAE modes increase with fast ion density and its gradient. In addition, lower n TAE modes, such as $n = 1$ can also be driven by energetic ions when off-axis heating with higher beam energy is employed in the experiment. The width of radial mode structures for lower n modes is usually wider than those for higher n modes. The perpendicular wave vector of the modes and Larmor radius of ions satisfy the relation $|k_\perp \rho_{\mathrm{Li}}|^2 \ll 1$. Finally, the polarization of the mode shows that the perturbed parallel electric field is much smaller than the electrostatic parallel electric field.

Keywords: energetic ions, TAE instability, simulation, GTC code

(Some figures may appear in colour only in the online journal)

1. Introduction

Shear Alfven waves commonly exist in tokamak plasmas. Two Alfven waves with the same toroidal mode number n but different poloidal mode numbers, for example m and $m + 1$, can strongly couple at the position of safety factor $q = (m + 0.5)/n$ and create a frequency gap where the continuum damping can be weakened dramatically. The toroidicity-induced Alfven eigenmode (TAE) located in the frequency gap was first predicted in theory [1]. In general, TAE is stable in the absence of

strong driving sources, such as neutral beam injection (NBI) heating, alpha particles from the fusion product [2–9]. The excitation mechanism of TAE mainly comes from the resonant interaction between wave and energetic particles (EPs). When the density gradient of EPs is high enough to overcome the electron/ion Landau damping [2, 3] and the continuum damping [10], TAE modes can be driven by EPs with velocity $v_{//} = v_A/(2k+1)$ ($k = 0, 1, 2\ldots$). In particular, TAE modes driven by EP beam with a one-third Alfven speed are extensively observed in experiment. In many auxiliary heating experiments, for example, NBI, ECRH/ICRH (electron/ion cyclotron resonant heating), LH (lower hybrid wave heating) and so on, TAE modes are extensively observed [11–13]. The TAE instabilities often induce large fast particles loss and eject a great amount of EPs which can damage first wall of vacuum cell of tokamak. Consequently, the heating efficiency as well as the confinement of plasmas can be degraded dramatically due to fast particles loss [14–16].

Gyrokinetic simulations using the gyrokinetic toroidal code (GTC) have been applied to investigate the nonlinear properties of turbulent transport regulated by zonal flow [17]. Since then, many functions of the GTC code have been developed to study both micro-instabilities and macro-instabilities, for example, the gyrokinetic simulations of TAE [18–20], the beta-induced Alfven eigenmode (BAE) [21, 22], the geodesic acoustic mode (GAM), the reversed shear Alfven eigenmode (RSAE) [23–25], as well as the electrostatic turbulence [26, 27]. Contrary to the predictions of conventional MHD theory, the mode structures of TAE simulated with GTC code are much narrower and their radial symmetries are usually broken due to the non-perturbation kinetic contribution of EPs [18–20]. Compared with previous TAE simulations [18–20], this work focuses on interpreting the experimental phenomenon observed on HL-2A tokamak and acquiring information with regard to energetic ions from the simulation, such as the fractions of energetic ions, the critical density of energetic ions for exciting TAE modes and the dominant energetic ions, trapped or passing to drive the TAE modes. The TAE instabilities induced by EPs are located at the positions of maximum EP pressure gradient where the mode structures of TAE are highly localized [20]. Just like other MHD instabilities, the excited TAE modes can easily induce fast particle losses which are observed in many tokamak devices [15, 28, 29, 30, 31]. The TAE activities have also been measured on HL-2A tokamak to degrade plasma confinement [31]. However, in current HL-2A auxiliary heating experiment, the density profile of EPs cannot be measured, which hinder us from studying the properties of MHD instabilities correlated with EPs. On the other hand, for HL-2A parameters, the TAE modes with low mode numbers, such as $n = 1, m = 1$ are difficult to excite due to weak driving forces, non-negligible damping as well as the mismatching between thermal velocity of EPs and Alfven speed. Consequently, these low n (m) modes have not been observed in HL-2A experiment. Therefore, the main motivations for performing the simulations reported in this paper are as follows, (i) to find out the possible amount of energetic ions and the corresponding critical density for inducing TAE modes in HL-2A plasmas, (ii) to simulate the properties of the TAE modes, such as the mode radial and poloidal structures, the eigen-frequencies as well as the linear growth rates, and (iii) to investigate the excitation requirement of low n (m) TAE modes.

This paper is organized as follows. In section 2, the physical equations for gyrokinetic simulations are given. The configuration of HL-2A, the plasma parameters and the simulated results are presented in section 3, and the main results are summarized in section 4.

2. The physical model for gyrokinetic simulation

GTC is a particle-in-cell code for simulation of turbulence, transport and MHD instabilities in magnetic fusion plasmas. The global field-aligned mesh and parallel elliptic solvers via PETSc are employed. The gyrokinetic formulations to simulate TAE by GTC code in 5D frame $(\vec{X}, \mu, v_{//})$ are written as follows [18, 19, 21, 32],

$$[\frac{\partial}{\partial t} + \dot{\vec{X}} \cdot \nabla + \dot{v}_{//} \frac{\partial}{\partial v_{//}} - C_\alpha] f_\alpha = 0 \tag{1}$$

$$\dot{\vec{X}} = v_{//} \frac{\vec{B}}{B_0} + \vec{v}_E + \vec{v}_c + \vec{v}_g, \tag{2}$$

$$v_{//} = -\frac{1}{m_\alpha} \frac{\vec{B}^*}{B_0} \cdot (\mu \nabla B_0 + Z_\alpha \nabla \Phi) - \frac{Z_\alpha}{m_\alpha c} \frac{\partial A_{//}}{\partial t}. \tag{3}$$

Here, the subscript α represents the species of electrons, thermal ions and energetic ions. m_α and Z_α are particle mass and electric charge number, respectively. The variables $\vec{X}, \mu, v_{//}$ are, respectively, gyrocenter position, magnetic moment and parallel velocity of particles. C_α is the collision operator which is neglected in this work for the collisionless plasmas being considered. f_α is the distribution function of particles. ϕ is the electrostatic potential and $A_{//}$ is the parallel component of vector potential. In our description, the compressional component of magnetic field perturbation is excluded by assuming $\delta B_{//} = 0$. Thus, the perturbed magnetic field is only contributed by the perpendicular component, that is $\delta \vec{B} = \delta \vec{B}_\perp = \nabla \times (A_{//} \vec{b}_0)$. The equilibrium magnetic fields are expressed by $\vec{B}_0 = B_0 \vec{b}_0$. Here, the vector $\vec{b}_0$ is defined with $\vec{b}_0 = \vec{B}_0/B_0$. The total magnetic field $\vec{B}$ in equations (2) and (3) is given by $\vec{B} = \vec{B}_0 + \delta \vec{B}$. The $\vec{E} \times \vec{B}$ drift velocity $\vec{v}_E$, the curvature drift velocity $\vec{v}_c$ and the magnetic gradient drift velocity $\vec{v}_g$ are expressed as following, respectively,

$$\vec{v}_E = \frac{c \vec{b}_0 \times \nabla \phi}{B_0}, \tag{4}$$

$$\vec{v}_c = \frac{v_{//}^2 \nabla \times \vec{b}_0}{\Omega_\alpha}, \tag{5}$$

$$\vec{v}_{\rm g} = \frac{\mu \vec{b}_0 \times \nabla B_0}{m_\alpha \Omega_\alpha}. \tag{6}$$

Here, Ω_α stands for the cyclotron frequencies of electrons, thermal ions or energetic ions, respectively. In this work, we focus on simulating TAE instability induced by energetic ions from NBI on HL-2A. Thus, in order to overcome the difficulty from numerical calculation, we use the fluid-kinetic hybrid electron model [33] which is consist of lowest order adiabatic part described with fluid equations and higher order non-adiabatic response treated kinetically. The lowest order adiabatic part can be readily obtained by integrating over equation (1) to get the following continuity equation of the thermal electron density,

$$\frac{\partial \delta n_{\rm e}}{\partial t} + \vec{B}_0 \cdot \nabla \frac{n_{\rm e_0} \delta u_{\rm e_{//}}}{B_0} + B_0 \vec{v}_{\rm E} \cdot \nabla \left(\frac{n_{\rm e_0}}{B_0}\right) - n_{\rm e_0} (\vec{v}_{\rm e^*} + \vec{v}_{\rm E}) \cdot \frac{\nabla B_0}{B_0} = 0. \tag{7}$$

Here, $\vec{v}_{\rm e^*} = \vec{b}_0 \times \nabla (\delta p_{\rm e_{//}} + \delta p_{\rm e\perp})/(n_{\rm e_0} m_{\rm e} \Omega_{\rm e})$, $n_{\rm e_0} = \int f_{\rm e_0} {\rm d}^3 v$, $\delta p_{\rm e_{//}} = \int \delta f_{\rm e} m v_{//}^2 {\rm d}^3 v$, $\delta p_{\rm e\perp} = \int \delta f_{\rm e} \mu B_0 {\rm d}^3 v$. Here, $\delta u_{\rm e_{//}}$ in equation (7), the perturbed parallel velocity of the electrons can be obtained from Ampere's law,

$$\frac{c}{4\pi} \nabla_\perp^2 \delta A_{//} + \sum_{\alpha=i,f} Z_\alpha n_{\alpha 0} \delta u_{\alpha_{//}} = e n_{\rm e_0} \delta u_{//\rm e}, \tag{8}$$

here, the perturbed vector potential can be calculated by making use of the Faraday's law.

$$\frac{1}{c} \frac{\partial \delta A_{//}}{\partial t} = \nabla_{//} (\phi_{\rm eff} - \phi). \tag{9}$$

By expanding equation (1) for electrons and keeping the leading order of $\omega/k_{//} v_{//}$, we can obtain a zeroth order distribution function $\delta f_{\rm e}^0$ [32, 33]. Then, integrating over velocity and assuming the uniform thermal electron density, the effective potential $\phi_{\rm eff}$ can be obtained as follows,

$$\frac{e\phi_{\rm eff}}{T_{\rm e}} = \frac{\delta n_{\rm e}}{n_{\rm e_0}} - \frac{\delta \psi}{n_{\rm e_0}} \frac{\partial n_{\rm e_0}}{\partial \psi_0}, \tag{10}$$

where ψ_0 and $\delta\psi$ are the equilibrium and perturbed poloidal flux given in [21, 32, 33]. Thus, in the case of uniform thermal electron density profile, the perturbed electron pressure in equation (7) can be written $\delta P_{\rm e_{//}} = \delta P_{\rm e\perp} = e n_{\rm e_0} \phi_{\rm eff}$. Together with the above equations, the closed system can be formed by the gyrokinetic Poisson's equation,

$$\frac{Z_{\rm i}^2 n_{\rm i}}{T_{\rm i}} (\phi - \tilde{\phi}) = \sum_{\alpha=i,e,f} Z_\alpha \delta n_\alpha, \tag{11}$$

where $\tilde{\phi}$ is the gyrophase-averaged electrostatic potential.

3. Gyrokinetic simulation of TAE on the HL-2A tokamak

In this work, we simulate the TAE instabilities observed in HL-2A NBI heating experiment by using GTC code and investigate the linear properties of TAE modes excited by energetic ions. The main HL-2A experimental parameters

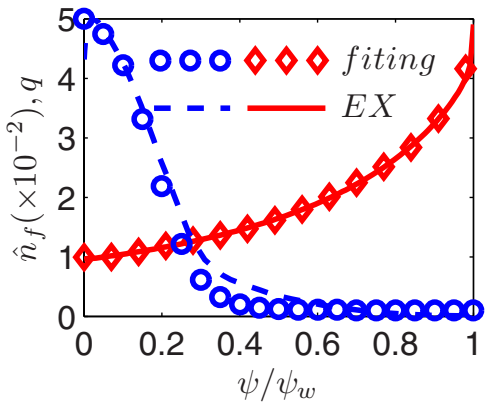

Figure 1. The safety factor q (red lines) and fast ions density (blue lines) profiles as functions of magnetic flux, the red solid and blue dashed lines are the experimental safety factor and fast ion density profiles of HL-2A tokamak calculated with EFIT and NUBEAM codes whereas the red diamonds and blue circles represent polynomial and analytical fit.

are as follows. The minor radius $a = 40$ cm, the major radius $R_0 = 165$ cm, the toroidal magnetic field at the major radius $B_{0\rm t} = 1.39$ T, the plasma current $I_{\rm p} = 150$ kA, the density of electrons $n_{\rm e} = 2$–$3(\times 10^{19})$ m^{-3} during NBI heating [12], the thermal particles temperature $T_{\rm e} = T_{\rm i} = 1$ keV, the temperature ratio of energetic ions to thermal electrons is $T_{\rm f}/T_{\rm e} = 40$. The Alfven speed is $v_{\rm A} = B_{\rm t}/\sqrt{4\pi n_{\rm i} m_{\rm i}}$ and $n_{\rm i}$, $m_{\rm i}$ are density and mass of thermal ions, respectively. The Alfven frequency $\omega_{\rm A} = k_{//} v_{\rm A}$ and the parallel wave vector $k_{//} = (n - m/q)/R_0$, where q is the safety factor.

3.1. Profiles of safety factor and energetic ions on HL-2A

Profiles safety factor and density of energetic ions are important for the excitation of TAE instabilities. The former influences frequency gap of continuous spectrum, whereas the latter is related to main driving source for TAE modes. Therefore, in order to simulate HL-2A experimental results as accurate as possible, the safety factor and the spatial profile of energetic ions are loaded from the experiment data calculated with EFIT and NUBEAM codes. However, the distribution function of the energetic ions is loaded with an isotropic Maxwellian distribution in phase space. Shown in figure 1 are the profiles of safety factor and energetic ions density as functions of normalized magnetic flux, calculated based on HL-2A experimental configurations. In order to carry out the gyrokinetic simulations using GTC code, conveniently, a polynomial $q = \sum_{k=0}^{6} c_k \hat{\psi}^k$ was employed to fit the experimental profile (the red solid line) and the result is given with the red diamonds in figure 1. Here, the normalized poloidal magnetic flux $\hat{\psi} = \psi/\psi_w$, where ψ_w is the magnetic flux at plasma boundary, the coefficients c_k are given as following, $c_0 = 0.99\,417$, $c_1 = -1.11\,906$, $c_2 = 24.007$, $c_3 = -104.56$, $c_4 = 220.56$, $c_5 = -215.19$, $c_6 = 79.844$. In addition, it is difficult to measure the density profile of energetic ions in the experiment at present stage. Thus, according to NBI heating condition deployed on the HL-2A tokamak, the density profile of energetic ions was calculated with NUBEAM code and

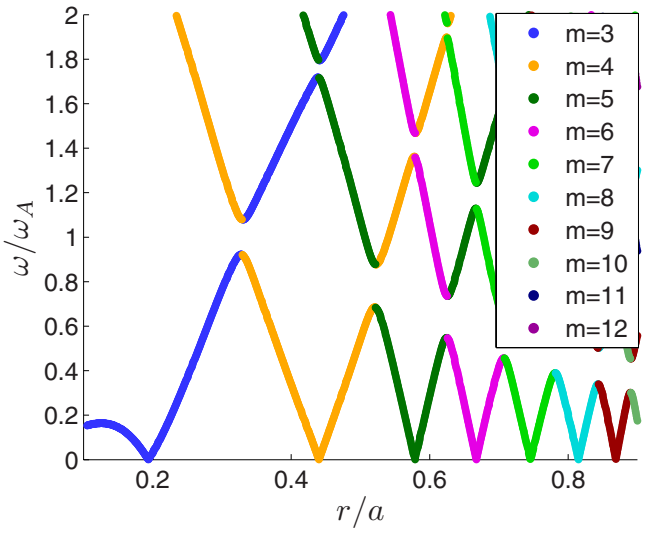

Figure 2. The normalized Alfven continua of $n = 3$ in the case of zero-β limit based on HL-2A experimental configuration. Here, ω_A refers to the Alfven frequency at the position of $q = 1.167$ and the same in figures 4 and 5.

presented by the dashed line in figure 1. Similar to the safety factor profile, a hyperbolic function of the normalized magnetic flux (the circles) was employed to fit the density profile of energetic ions (i.e. the dashed line) in figure 1 and given by the following equation,

$$\hat{n}_f = \hat{n}_{f0}\frac{1 + n_H\{\tanh[(\hat{\psi}_0 - \hat{\psi})/\Delta] - 1\}}{1 + n_H[\tanh(\hat{\psi}_0/\Delta) - 1]}, \qquad (12)$$

where $\hat{\psi}_0$ represents the position of maximum density gradient of energetic ions, the density profiles of fast ions with NBI on/off-axis heating can be usually realized by modifying the parameter $\hat{\psi}_0$. The index Δ is used to describe the density gradient of energetic ions and n_H represents the difference between maximum and minimum in the profile. The density of energetic ions is normalized to thermal electron density at the magnetic axis, i.e. $\hat{n}_f = n_f/n_{e_0}$. The variable $\hat{n}_{f0}$ is the normalized density of energetic ions on the magnetic axis. The measured electron density on HL-2A refers to line-averaged electron density in the middle plane. Since the frequency gap of Alfven continuous spectrum with toroidal mode number $n = 3$, poloidal mode numbers $m = 3/4$ is just in the vicinity of the magnetic axis and the radial variation of plasma density between magnetic axis and the frequency gap is small, a uniform plasmas density profile was used in the simulation.

3.2. Simulation of TAEs observed in HL-2A experiment

TAE modes, essentially being a shear Alfven wave, can only exist within the frequency gap of the Alfven continuous spectrum in toroidal geometry and are located at certain positions in the radial direction. The shear Alfven continuous spectrum as well as the corresponding frequency gaps can be conveniently determined by the ALCON code [24]. The curves shown in figure 2 are the Alfven continuous spectrum as functions of normalized minor radius, which are plotted in terms of HL-2A experimental configuration in the case of zero β (=pressure of thermal particles/magnetic pressure) limit calculated with ALCON code. The toroidal mode number $n = 3$ and the poloidal mode number m is in the range of 3–12. The first-order frequency gap can be formed when the poloidal harmonic $m = 3$ coupled with $m = 4$, whereas the higher order frequency gaps, for example the coupling of $m = 3$ and $m = 5$, 6 are neglected due to the fact that the ellipticity/triangularity-induced Alfven eigenmode (EAE/NAE) exist in these higher order frequency gaps [34]. From the blue and orange lines in figure 2, we learn that the first-order frequency gap is approximately located at the position of 1/3 minor radius. The radial position of the frequency gaps for $n = 2$ ($m = 2/3$) and $n = 1$ ($m = 1/2$) can be approximately estimated as located at the radial positions where $q = 1.25$ and $q = 1.5$, respectively. The TAE modes can be excited by EPs within these gaps. In this simulation work, we use 64 grid points in the radial direction, 128 grid points in the poloidal direction and 16 grid points in parallel direction. The number of particles per cell has been tested for convergence. For a typical run, there are 100 particles per cell for fast ions and 50 particles per cell for thermal ions, respectively. The time step size is $\Delta t = 0.005R_0/v_{A0}$.

The matching of the toroidal precession and bounce/transit frequencies of energetic ions as well as the linear combination of these characteristic frequencies with the Alfven frequencies at the gap positions provide two necessary conditions for the excitation of TAE mode. Note, here the concept of gap position refers to the radial locations of accumulation point where two Alfven continua with poloidal mode numbers m and $m + 1$ intersect and couple to each other. Although the damping is relatively weak in the gaps, the TAE modes are still stable in the absence of driving sources, e.g. fast particles or antenna excitation. When the pressure gradient of fast particles in the gap is strong enough, the TAE modes can be excited. As a result, the growth rates of the modes are approximately linear functions of the diamagnetic drift frequency of fast particles [35]. Theoretically, the TAE eigen-mode consists of many poloidal harmonics, but only the mth poloidal harmonic with relatively weaker damping is usually easy to be excited at the radial position where the condition $nq = m + 0.5$ is satisfied. Thus, the mode frequency of TAE is roughly equal to Alfven frequency at the position of $q(r) = (m + 0.5)/n$ where the vector potential of the mode has maximum and quickly decreases to zero outward. The radial mode structure of TAE is roughly Gaussian-like distribution profile. In general, the width of the radial mode structure is related to the magnetic shear values at the frequency gap positions and the pressure gradient of the energetic ion.

The neutral beam of HL-2A can be easily injected into the core plasma region due to relatively lower plasma density. As a result, the position of NBI deposition is roughly on the magnetic axis (i.e. on-axis heating). At the same time, it can be seen from the result shown in figure 2 that the frequency gap of the mode with $n = 3$, $m = 3/4$ is approximately located in the vicinity of the magnetic axis. Especially, when the parameters in equation (12) is set as $n_H = 0.49$, $\hat{\psi}_0 = 0.18$ and $\Delta = 0.11$, the hyperbolic function can approximately fit the

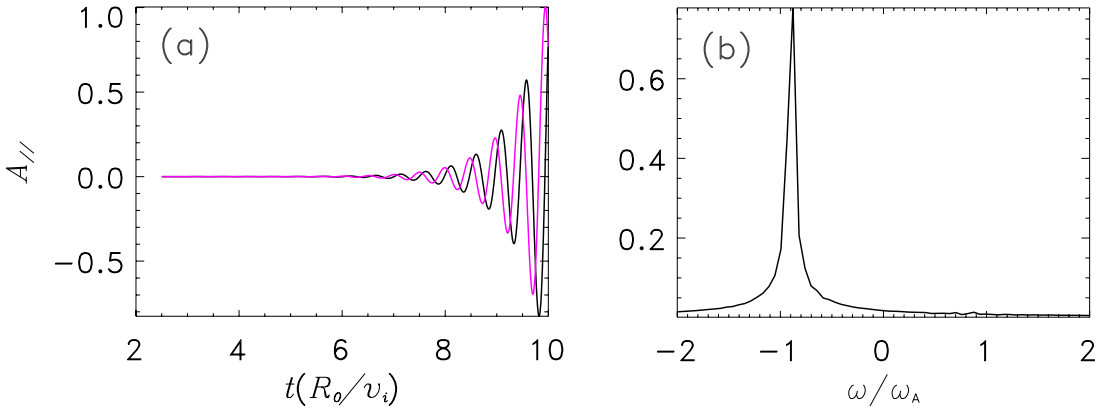

Figure 3. The time evolution of vector potential $A_{//}$ (a) and the frequency spectrum of $A_{//}$ (b) for TAE excited by fast ions in HL-2A with mode number $n = 3$, $m = 3/4$, beam ion energy $T_f = 40$ keV, the normalized magnetic flux $\hat{\psi}_0 = 0.18$ and the density ratio of fast ions to electrons $\hat{n}_{f0} = 0.05$. Here, v_i in the horizontal labels stands for thermal ion speed and the same in figures 9 and 11.

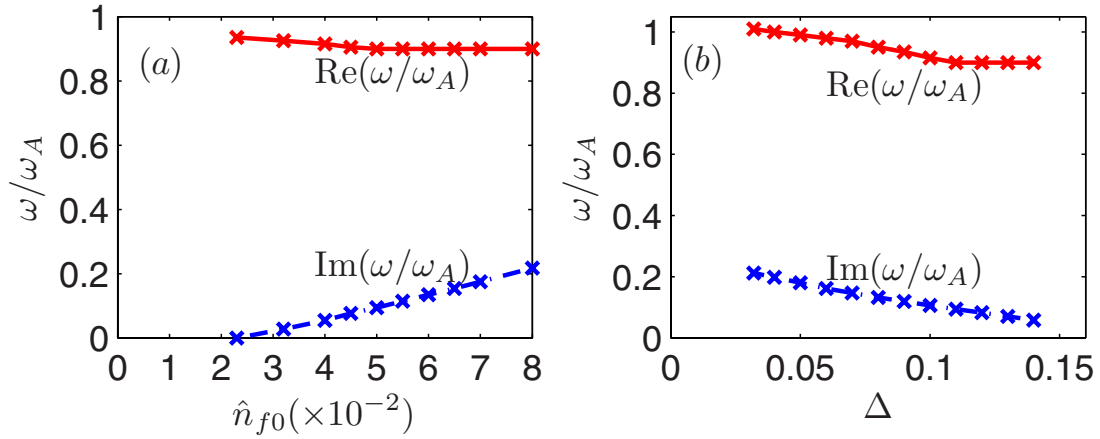

Figure 4. The real frequencies (red solid lines) and growth rates (blue broken lines) of TAE modes as functions of density (a) and the index of density profile (b) of energetic ions with mode number $n = 3$ and $m = 3/4$, beam ion energy $T_f = 40$ keV and the normalized magnetic flux $\hat{\psi}_0 = 0.18$. Here the crosses represent the data points.

blue dashed line shown in figure 1 and describe on-axis NBI heating. The ratio of the densities of energetic ions to thermal electrons at magnetic axis is $n_{f0}/n_{e0} = 0.05$. The simulated results are presented in figure 3, where the lines in figure 3(a) are the time evolution of vector potential $A_{//}$ of TAE modes. The black and pink lines are real and imaginary parts of vector potential, respectively. These curves show that, during the linear stage, the perpendicular magnetic field perturbation of TAE instability grows exponentially with growth rate $0.09\omega_A$. The line shown in figure 3(b) is the frequency spectrum of the vector potential which is normalized to Alfven frequency and obtained by Fourier transformation from the results in figure 3(a). This spectrum indicates that the real frequency of TAE mode is equal to $0.9\omega_A$, ten times of the growth rate. According to the parameters of HL-2A device, the real frequency of TAE mode is 211 kHz which is quantitatively in agreement with the experimental observation presented in figure 1(g) in [12].

In current experimental stage of the HL-2A tokamak, it is difficult to measure the fraction of EPs directly. Therefore, one of the main tasks to perform this simulation work is to find out the rough fraction of energetic ions as well as their critical density to excite TAE instabilities during NBI heating. Shown in figures 4(a) and (b) are the real frequencies (red solid lines) and growth rates (blue broken lines) of TAE modes as functions of normalized density and density gradient of energetic ions, respectively. Meanwhile, the density of fast ions and the mode frequencies are normalized to thermal electron density and Alfven frequency on magnetic axis, respectively. Moreover, the data points in figure 4 are marked with crosses, and the same in figure 5. The results show that the TAE instabilities can be excited when the density of fast ions is higher than a critical value ($\hat{n}_{f0} = 0.023$). The growth rate of the mode increases with increasing density of fast ions. The corresponding real frequency of TAE mode changes with the density of fast ions with a range similar to the growth rate, which is typical of eigen-modes. In addition, the lines shown in figure 4(b) present the dependence of real frequency and growth rate of TAE mode on Δ, the index of density profile used to scale the density gradient of fast ions. In this density profile model, the density gradient of fast ions increases with decreasing Δ. It can be learnt from the figure that TAE instabilities can be induced only when the gradient of fast ions is higher than a critical value. Moreover, the growth rate of the

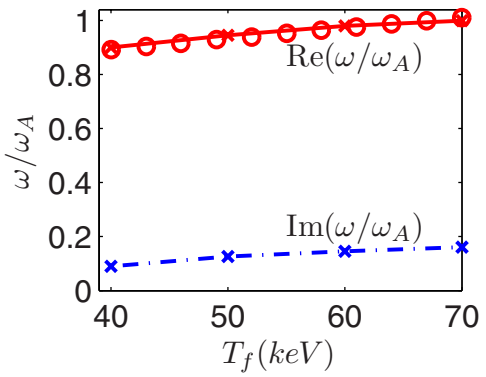

Figure 5. The real frequency (red solid line with crosses and red circles) and growth rate (blue broken line with crosses) as functions of beam ion energy (temperature) of energetic ions with mode number $n = 3$ and $m = 3/4$, the normalized magnetic flux $\hat{\psi}_0 = 0.18$, the density ratio of fast ions to thermal electrons $\hat{n}_{\mathrm{f0}} = 0.05$. Here, the crosses represent the data points.

mode increases with the EP density gradient. The result in figure 4(*a*) indicates that the normalized critical density of fast ions is around 0.023. Consequently, the fraction of energetic ions in HL-2A device should be higher than this value. The calculated results show that fine mode structures observed in experiments (not given here) can be obtained when the normalized density of energetic ions satisfies $\hat{n}_{\mathrm{f0}} = 0.03$. Therefore, the fraction of energetic ions in HL-2A experiment is approximately 3%. The critical density of energetic ions can also be analytically estimated according to the TAE theory given in [2], i.e. $\hat{n}_{\mathrm{f,crit}} = \frac{2T_{\mathrm{e}}v_{\mathrm{A}}/v_{\mathrm{e}}}{T_{\mathrm{f}}(2\omega_{*\mathrm{h}}/\omega_{\mathrm{A}}-1)F(x)}$. Here, v_{e} is thermal speed of electrons, $\omega_{*\mathrm{h}}$ is diamagnetic frequency of energetic ions and can be readily calculated by using equation (12). Note, it is convenient to use the relation $\mathrm{d}n_{\mathrm{f}}/(n_{\mathrm{f}}\mathrm{d}r) \approx \varepsilon B_{\mathrm{t}}\mathrm{d}n_{\mathrm{f}}/(n_{\mathrm{f}}\mathrm{d}\psi)$ when calculating the density gradient of energetic ions at the radial position of accumulation point, and the magnetic field value at this position is $B_{\mathrm{t}} = 1.28$ T which can be easily calculated from the equation $B_{\mathrm{t}} = B_{0\mathrm{t}}/(1 + r/R_0)$. The function $F(x) = x(1 + 2x^2 + 2x^4)\exp(-x^2)$ with $x = v_{\mathrm{A}}/v_{\mathrm{f}}$. By substituting the corresponding parameters into the above equation of energetic ions critical density, we can obtain the normalized critical density of energetic ions $n_{\mathrm{f,crit}} = 0.026$ which is very close to the simulated value 0.023. It should be pointed out that with respect to the analytical critical EI density given above, only the Landau damping is included in the model while other damping mechanisms are neglected due to the following reasons. (i) The radiative damping usually increases with poloidal mode numbers. For low poloidal mode number TAE modes ($m = 3$, 2, 1), the contribution of radiative damping is not important. (ii) For HL-2A low density plasmas, the collisional damping can also be neglected. Thus, the critical EI density to induce TAE may be slightly higher than the above estimation when all kinds of dampings are included. However, according to the analytical estimation in [36], the continuum damping is roughly 5% in the case of HL-2A parameters. Thus, analytical threshold density of energetic ions is closer to the simulation value 0.023 in the presence of continuum damping.

It is helpful for understanding the resonant excitation mechanism of TAE modes and determining the dominant energetic ions (e.g. trapped/passing ions) in inducing the modes to study the dependence of eigenfrequency on temperature (beam energy) of energetic ions. In general, the resonant requirements satisfy the relation $n\omega_{\mathrm{dh}} + l\omega_{\mathrm{b,t}} = \omega_{\mathrm{r}}$. Here, the variables ω_{r}, ω_{dh} and $\omega_{\mathrm{b,t}}$ represents the real frequency of TAE mode, the toroidal precession frequency, and the bounce/transit frequency of fast trapped/passing particles, respectively. The integer l is taken as $l = 0, \pm1, \pm2\ldots$. The toroidal precession and bounce/transit frequencies of energetic ions are given by the following equations, respectively [37–39],

$$\omega_{\mathrm{dh}} = \frac{qE}{r\,|e|\,BR_0}\begin{cases}\frac{2\mathrm{E}(k)}{\mathrm{K}(k)} - 1 + 4s\left[\frac{\mathrm{E}(k)}{\mathrm{K}(k)} - 1 + k^2\right] \\ 1 + 2k^2\left[\frac{\mathrm{E}(k_{\mathrm{p}})}{\mathrm{K}(k_{\mathrm{p}})} - 1 + s\left(\frac{2\mathrm{E}(k_{\mathrm{p}})}{\mathrm{K}(k_{\mathrm{p}})} - \frac{\pi\sqrt{1-k_{\mathrm{p}}^2}}{\mathrm{K}(k_{\mathrm{p}})}\right)\right]\end{cases},$$
$$\omega_{\mathrm{b,t}} = \frac{\pi}{qR_0}\sqrt{\frac{\varepsilon\alpha E}{m_{\mathrm{h}}}}\begin{cases}\frac{1}{2\mathrm{K}(k)} \\ \frac{k}{\mathrm{K}(k_{\mathrm{p}})}\end{cases}. \quad (13)$$

Here, K and E are the first and second kinds of elliptic functions with the argument $k^2 = (1/\alpha - 1 + \varepsilon)/2\varepsilon$ and $k_{\mathrm{p}} = 1/k$. ε is the local inverse aspect ratio, α is the pitch angle of energetic ions, E and m_{h} are the energy and mass of fast ions, and s is the magnetic shear. The neutral beam is injected into the plasma at an angle of 42° along the tangential direction in HL-2A tokamak. Thus, the pitch angle $\alpha = (v_{\perp}/v)^2 = 0.4477$ in this device, which means that passing energetic ions are dominant. According to the parameters at the gap position, $\varepsilon = 0.0848$, $s = 0.4569$, the integers $n = 3$ and $l = 1$, we can estimate the frequency of TAE mode according to the resonant relation given above, $f_{\mathrm{TAE}} = \omega_{\mathrm{r}}/2\pi = 203$ kHz which is in agreement with the simulation results. On the other hand, the fraction of trapped particles is proportional to $\sqrt{2\varepsilon}$ (~0.41 at the frequency gap position for HL-2A). As a result, the fraction of trapped fast ions in HL-2A is also significant. The highest ω_{dh} and ω_{b} can be obtained when we set the elliptical function argument $k = 0$ (deeply trapped ions). Meanwhile, the corresponding mode frequency is $f_{\mathrm{TAE}} = \omega_{\mathrm{r}}/2\pi = 125$ kHz for $n = 3$, $l = 1$, much less than the eigenfrequency of the TAE mode. But for higher l harmonic, for example, $n = 3$, $l = 3$, it is difficult to excite TAE modes by trapped energetic ions due to lower beam injection energy and tangential NBI injection, although the resonant condition seems to be satisfied and the corresponding eigen-frequency $f_{\mathrm{TAE}} = \omega_{\mathrm{r}}/2\pi = 213$ kHz. Consequently, TAE modes are mainly excited by passing fast ions. The lines shown in figure 5 are real frequency (red solid line with crosses and red circles) and growth rate (blue broken line with crosses) as functions of temperature (beam energy) of energetic ions. The red circles are a nonlinear function of fast ion temperature, $\omega_{\mathrm{r}} = aT_{\mathrm{f}} + b\sqrt{T_{\mathrm{f}}} + c$ with $a = 0.0035$, $b = 0.00\,665$ and $c = 0.71$, used to fit the real frequency (red solid line). It can be learnt from the solid line and the red circles that the real frequency of TAE mode can be perfectly fitted by the analytical function, which analytically demonstrates that the real frequency of the TAE mode is just the linear combination of toroidal precession frequency and transit frequency of passing fast ions, and the toroidal precession and the transit

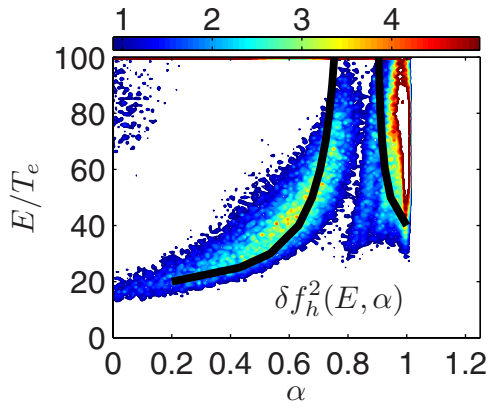

Figure 6. The contour plot of $|\delta f_h|^2$ in the phase space of energy E and pitch angle α of fast ions. The bold black lines indicate the resonant conditions $n\omega_{\rm dh} + l\omega_{\rm b,t} = \omega_{\rm TAE}$.

motions of energetic ions are dominant for resonant excitation of TAE modes. Therefore, the transit energetic ions play an important role in exciting TAE modes in HL-2A tokamak. In addition, owing to diamagnetic drift frequency being directly proportional to the temperature, the growth rate of the TAE mode increases with beam energy.

In addition, the resonant condition can also be identified in the phase space from the simulation results of $|\delta f_h|^2 \sim (E, \alpha)$, and the corresponding contours are shown in figure 6. Here, the variable δf_h represents perturbed distribution function of energetic ions. Meanwhile, the bold black lines are the analytical resonant condition ($n\omega_{\rm dh} + l\omega_{\rm b,t} = \omega_{\rm TAE}$, $n = 3$, $l = 1$ for passing EIs and $n = 3$, $l = 3$ for trapped EIs) calculated according to equation (13). The results show that two resonant zones are in the range of $0.2 < \alpha < 0.8$, $20 < E < 100$ (keV) and $0.9 < \alpha < 1.0$, $40 < E < 100$ (keV), respectively. Theoretically speaking, both trapped and passing energetic ions can destabilize TAE instabilities via resonant interaction between wave and particles. However, it is difficult for trapped energetic ions to excited TAE mode due to the tangential beam injection and lower maximum beam energy (around 40 keV) for HL-2A. Moreover, it can be seen from the phase space structures of $|\delta f_h|^2$ in figure 6 that the resonance only occurs in a narrow pitch angle range for the trapped fast ions. On the contrary, according to the maximum beam energy and the beam injection direction employed on HL-2A device, the resonant zone is usually located in small pitch angle and lower beam energy region. Therefore, the passing energetic ions are still dominant in HL-2A device to drive TAE instabilities.

Shown in figures 7(*a*) and (*b*) are the poloidal mode structures of electrostatic potential ϕ (a) and vector potential $A_{//}$ (b), whereas those in figure 7(*c*) and (*d*) are the radial mode structures of the counterparts with toroidal mode number $n = 3$ and poloidal mode numbers $m = 3$ (the red lines) and $m = 4$ (the blue lines). The dashed lines in figure 7(*d*) are the vector potential calculated by employing Faraday's law. By comparison of the poloidal mode structures of TAE mode at different time slice (the poloidal mode structure at another time slice is not given), it can be learnt that the mode propagates in the diamagnetic drift direction of fast ions. The radial mode structures of TAE indicate that the modes are localized within the frequency gap of Alfven continuous spectrum. Generally speaking, the ideal mode should satisfy two conditions. First, the perpendicular wave vector and Larmor radius of thermal ions satisfy the relation $|k_\perp \rho_{\rm Li}|^2 \ll 1$. Secondly, the parallel perturbed electric field is small, i.e. $\delta E_{//} \ll \vec{b}_0 \cdot \nabla\phi$ [40]. Based on the parameters of HL-2A tokamak, the first condition can be easily checked. On the other hand, the zero-perturbed parallel electric field condition can be checked by the polarization of TAE mode. As mentioned above, the vector potential can be analytically calculated by using Faraday's law, i.e. $\partial_t A_{//} = -c\vec{b}_0 \cdot \nabla\phi$ and presented with the dashed line in figure 7(*d*). The results shown in figure 7(*d*) indicate that the dashed lines are in approximate agreement with the solid lines, thus the perturbed parallel electric field $\delta E_{//} \ll \vec{b}_0 \cdot \nabla\phi$ is satisfied. Both conditions mentioned above show that the mode studied in this work is close to an ideal MHD branch and is typical of TAE mode. Besides, we can also demonstrate that the mode is an Alfven mode by checking the dependence of eigenmode frequency on electron density. Shown in figure 8 is the frequency of TAE mode as function of electron density. The solid line represents the simulation results and the red diamonds, being inversely proportional to square root of electron density, are employed to fit the solid line. The nearly perfect agreement between the simulation result (solid line) and analytical estimation (the red diamonds) indicates that the mode frequency satisfies the Alfven wave frequency scaling. At the same time, the simulation result (solid line) is also in agreement with the experimental measurements given in [12] where the inverse proportional dependence of mode frequency on square root of electron density was presented.

3.3. Conditions for excitation of low n TAE modes on HL-2A

Although TAE modes with mode number $n = 3$ ($m = 3/4$) have been observed in experiment and the mode frequency is in agreement with the simulated results, yet the lower n number modes, such as $n = 2$ ($m = 2/3$) and $n = 1$ ($m = 1/2$) have not been observed in HL-2A experiments. The reasons may include weak driving source, strong damping and the variation of resonant condition coming from changing of toroidal mode number. According to the resonance condition given in section 3.2 $n\omega_{\rm dh} + l\omega_{\rm t} = \omega_{\rm TAE}$, it can be seen that the original resonance condition may not be satisfied any longer when the mode number n is changed. To be specific, the low n TAE modes cannot be induced unless the beam energy is increased to raise the characteristic frequency (such as the toroidal precession frequency, the bounce/transit frequency of EIs) and satisfy the new resonance conditions. Besides, the positions of maximum density gradient of energetic ions also play a crucial role in destabilizing the TAE mode. Strong enough density gradient of energetic ions within the frequency gap is another important condition for driving TAE instabilities. The frequency gaps for low n modes, e.g. $n = 2$, $m = 2/3$ and $n = 1$, $m = 1/2$, can be roughly estimated from the TAE

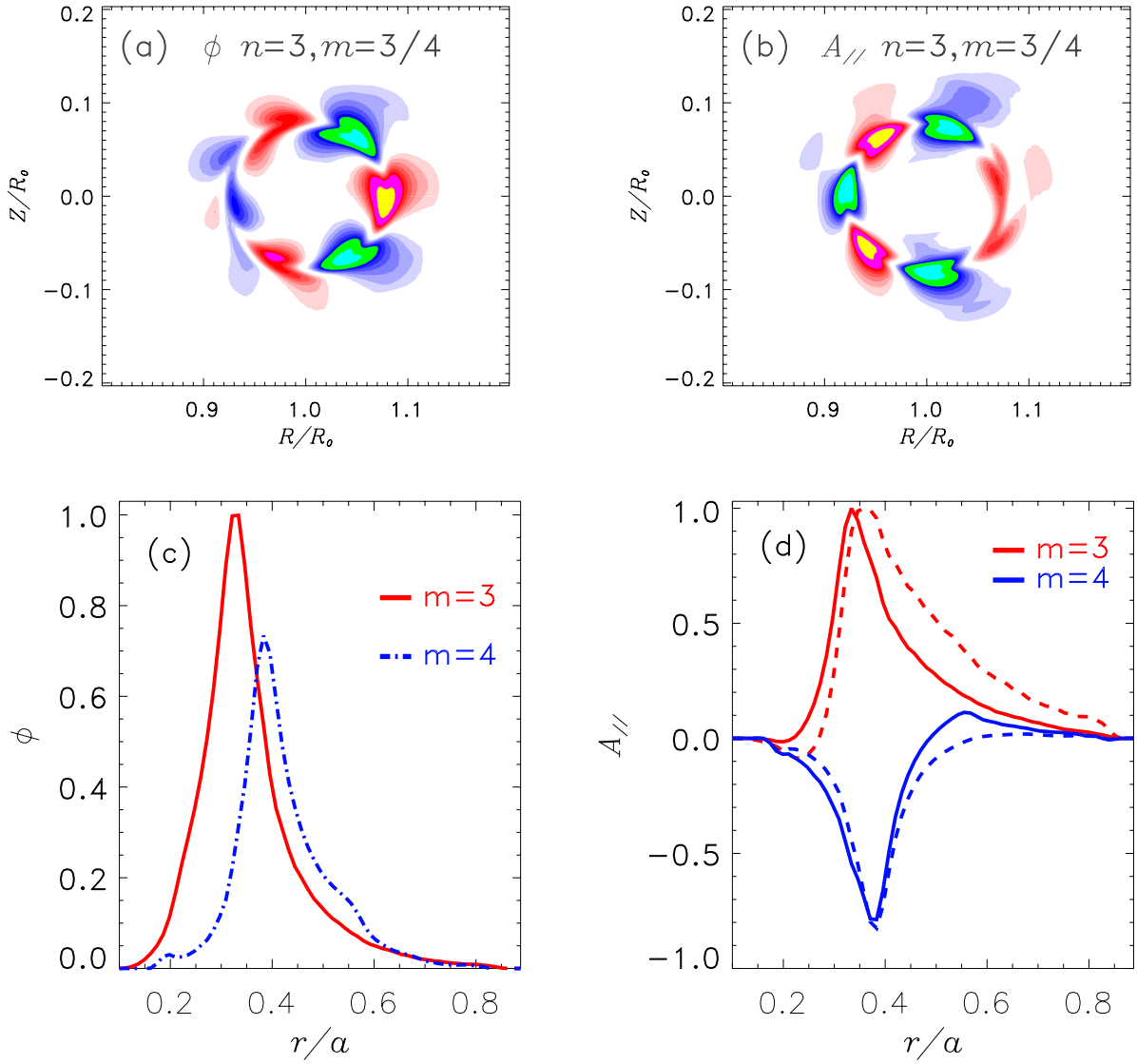

Figure 7. The poloidal ((*a*) and (*b*)) and radial ((*c*) and (*d*)) mode structures of electrostatic potential ϕ and vector potential $A_{//}$ for TAE induced by energetic ions in HL-2A tokamak with toroidal mode number $n = 3$ and poloidal mode numbers $m = 3/4$, beam energy $T_f = 40\,\text{keV}$ and the normalized magnetic flux $\hat{\psi}_0 = 0.18$, the density ratio of fast ions to thermal electrons $\hat{n}_{f0} = 0.05$. The dashed lines represent analytical calculations by Faraday's law.

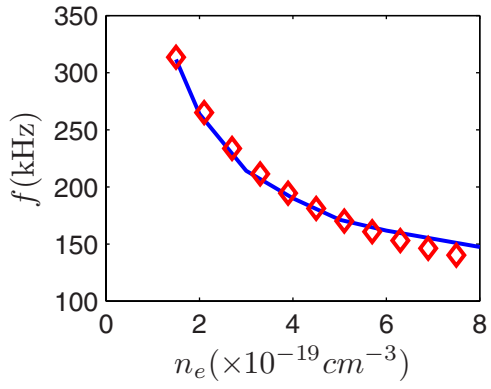

Figure 8. The mode frequency of TAE as functions of electron density, the solid line represents the simulation result with the GTC code and the red diamonds represent a function being proportional to $1/\sqrt{n_e}$.

theory [2] as located at the positions $\hat{\psi}_0 = 0.27$ and $\hat{\psi}_0 = 0.44$, respectively, for HL-2A parameters. Under the condition of on-axis NBI heating, the density gradients of energetic ions at the radial position of accumulation point for low n (especially $n = 1$) modes are correspondingly small, which weakens the driving force at these positions. On the other hand, considering the dependence of toroidal mode number n on resonant excitation requirement, the toroidal precession frequencies of energetic ions cannot match with the shear Alfven frequencies any longer at the gap position in low n cases. Both reasons may result in the failures to observe low n TAE modes in HL-2A experiment. Accordingly, the low n TAE modes may be excited through modification of the position of maximum density gradient of energetic ions and raising the injection energy of neutral beam. Theoretically, the resonance relation can be satisfied when the maximum beam energy (temperature of energetic ions) is raised to $T_f = 44\,\text{keV}$ and $T_f = 50\,\text{keV}$ for

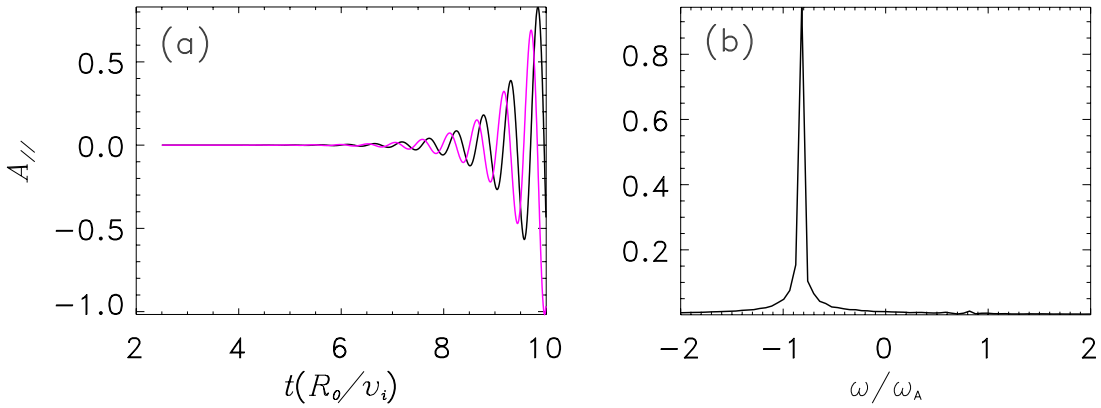

Figure 9. The time evolution of vector potential $A_{//}$ (a) and the frequency spectrum of $A_{//}$ (b) for TAE excited by fast ions in HL-2A with mode number $n = 2$, $m = 2/3$, beam energy $T_f = 40\,\mathrm{keV}$ and the normalized magnetic flux $\hat{\psi}_0 = 0.25$, the density ratio of fast ions to electrons $\hat{n}_{f0} = 0.05$.

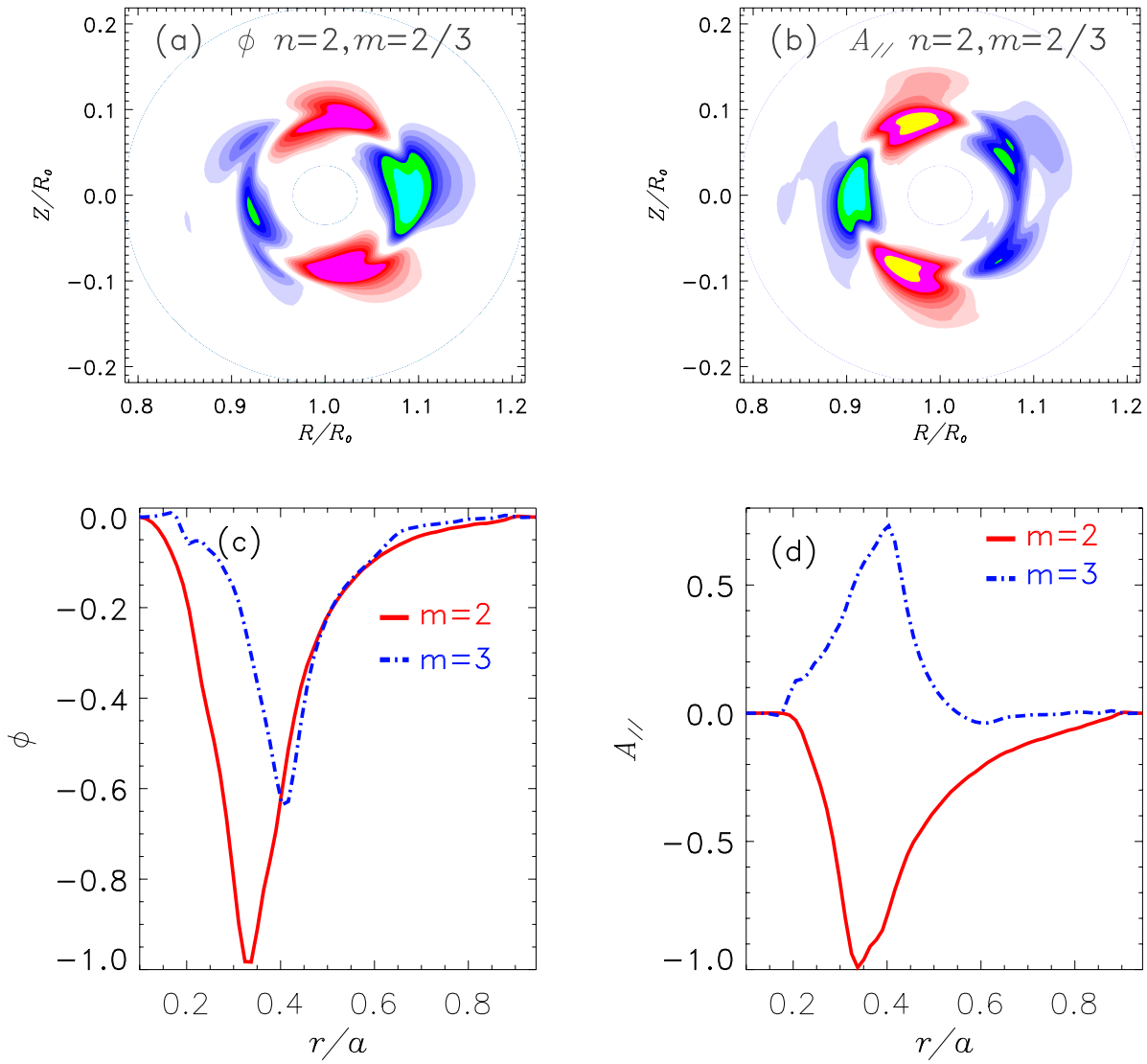

Figure 10. The poloidal ((*a*) and (*b*)) and radial ((*c*) and (*d*)) mode structures of electrostatic potential Φ and vector potential $A_{//}$ for TAE induced by energetic ions based on HL-2A tokamak parameters with toroidal mode number $n = 2$ and poloidal mode numbers $m = 2/3$, beam energy $T_f = 40\,\mathrm{keV}$ and the normalized magnetic flux $\hat{\psi}_0 = 0.25$, the density ratio of fast ions to electrons $\hat{n}_{f0} = 0.05$.

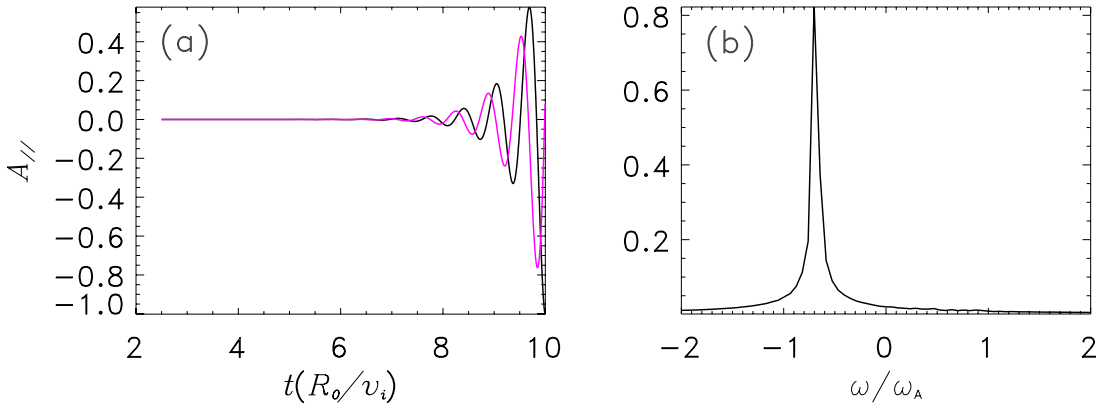

Figure 11. The time evolution of vector potential $A_{//}$ (a) and the frequency spectrum of $A_{//}$ (b) for TAE excited by fast ions in HL-2A with mode number $n = 1$ and $m = 1/2$, beam energy $T_f = 80$ keV and the normalized magnetic flux $\hat{\psi}_0 = 0.575$, the density ratio of fast ions to electrons $\hat{n}_{f0} = 0.05$.

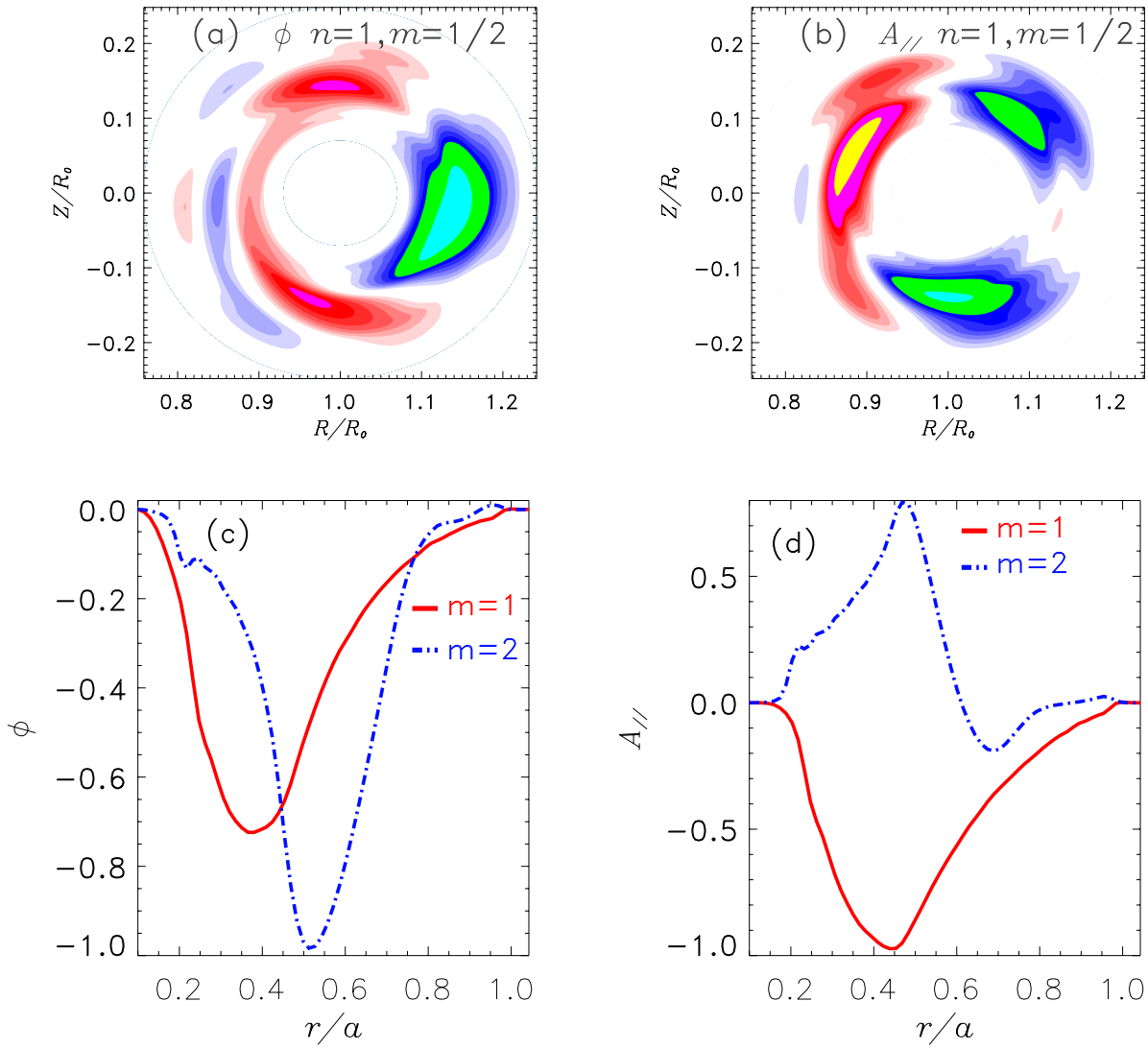

Figure 12. The poloidal (a), (b) and radial (c), (d) mode structures of electrostatic potential ϕ and vector potential $A_{//}$ for TAE induced by energetic ions based on HL-2A tokamak parameters with toroidal mode number $n = 1$ and poloidal mode numbers $m = 1/2$, beam energy $T_f = 80$ keV and the normalized magnetic flux $\hat{\psi}_0 = 0.575$, the density ratio of fast ions to electrons $\hat{n}_{f0} = 0.05$.

$n = 2$ and $n = 1$, respectively. At the same time, the positions of maximum density gradient need to be shifted to $\hat{\psi}_0 = 0.27$ and $\hat{\psi}_0 = 0.44$ for $n = 2$ and $n = 1$, respectively. Then, the low n modes, $n = 1$, $n = 2$ can also be induced by EPs. Note, these parameters about density profile and temperature of energetic ions are only theoretical estimations whereas the real values can be determined by simulation.

According to the above theoretical analysis, the temperature of energetic ions is first changed to $T_f = 44\,\mathrm{keV}$ for $n = 2$ and $T_f = 50\,\mathrm{keV}$ for $n = 1$, whereas the corresponding density profile is not changed. The simulated results show that the $n = 1$ mode cannot be excited by energetic ions at all. The $n = 2$ ($m = 2/3$) mode can be induced, but the mode structure is not well organized. For example, the amplitude of $m = 2$ is much larger than that of $m = 3$, which is not given here. It is necessary to modify the value of normalized magnetic flux $\hat{\psi}_0$ in equation (12), or to change the maximum injection energy of neutral beam so as to satisfy the resonant condition. Considering the little difference of resonance requirements for inducing $n = 2$ and $n = 3$ TAE modes, the maximum beam energy is still kept unchanged for $n = 2$ case, i.e. $T_f = 40\,\mathrm{keV}$. The TAE mode for $n = 2$ can be driven unstable and the results are presented in figures 9 and 10, when the normal magnetic flux in equation (12) is changed to $\hat{\psi}_0 = 0.25$ ($n_H = 0.49$, $\Delta = 0.11$). In accordance with the above analytical estimation, the mode with lower toroidal mode number, such as $n = 1$ ($m = 1/2$), can be driven unstable when the temperature of fast ions and the normalized magnetic flux are set to $T_f = 50\,\mathrm{keV}$ and $\hat{\psi}_0 = 0.44$, respectively. Furthermore, the TAE mode with $n = 1$ ($m = 1/2$) is excited and a perfect mode structure can be obtained when the temperature of fast ions $T_f = 80\,\mathrm{keV}$ and $\hat{\psi}_0 = 0.575$ ($n_H = 0.49$, $\Delta = 0.11$) are employed, respectively. The corresponding simulation results are shown in figures 11 and 12. Meanwhile, the results shown in figures 9 and 11 are evolution of vector potential $A_{//}$ and the corresponding frequency spectrums for TAE modes with lower mode numbers $n = 2$ ($m = 2/3$) (e.g. figure 9) and $n = 1$ ($m = 1/2$) (e.g. figure 11). Similar to figure 3, the black and pink lines are real and imaginary parts of vector potential, respectively. By comparing with those in figure 3, it can be learnt that the mode frequencies decrease with decreasing toroidal mode numbers. Thus, besides the results presented in figure 5, the contribution of toroidal precession resonance for the excitation of TAE instabilities is confirmed once again. Especially, for the case of $n = 1$, the maximum neutral beam energy has been changed to $T_f = 80\,\mathrm{keV}$ so as to match with the Alfven frequency and to satisfy the excitation requirement of TAE mode. Presented in figures 10 and 12 are the poloidal and radial mode structures for $n = 2$ ($m = 2/3$) and $n = 1$ ($m = 1/2$) modes, respectively. From the positions of both poloidal and radial mode structures of TAE, it can be seen that the modes shift outwards for lower toroidal mode number n and the radial width of the mode structure becomes larger. It has been pointed out that the width of mode structure increases with magnetic shear. Moreover, the magnetic shear value at the frequency gap position for $n = 1$ ($m = 1/2$) is bigger than those for $n = 2$ ($m = 2/3$) and $n = 3$ ($m = 3/4$). Thus, the radial distribution of the TAE mode structure is nearly global (see figure 12), which may be resulted from the large magnetic shear value at the frequency gap position for $n = 1$ case.

4. Conclusions

The TAE excited by energetic ions was observed in HL-2A NBI experiment. The numerical simulation has been first performed by using GTC code. It is found that TAE modes can be excited by fast ions when the ratio of densities of fast ions to the electrons of background plasmas is higher than a critical value ($n_{f0}/n_{e0} \sim 0.023$) which is very close to the theoretical prediction of 0.026, showing a reasonable agreement with analytic TAE theory. The fraction of energetic ions in HL-2A experiment is approximately 3%. The growth rates of TAE modes increase with increasing of both the density and its gradient of fast ions. The TAE frequency is around 211 kHz and inversely proportional to the square root of electron density, which is quantitatively in agreement with the experimental observation. In addition, the frequency of TAE modes is in resonance with the combination of toroidal precession and transit frequencies of energetic passing ions, and increases with temperature of energetic ions (beam energy) in accordance with the relation $\omega_r = aT_f + b\sqrt{T_f} + c$, which indicates that the resonances with toroidal precession and transit of energetic ions play an crucial role in inducing TAE mode. Meantime, the phase space structures of $|\delta f_h|^2$ show that the TAE modes are mainly excited by passing energetic ions instead of by trapped energetic ions based on the parameters of HL-2A. The perpendicular wave vector and Larmor radius of ions satisfy the relation $|k_\perp \rho_{Li}|^2 \ll 1$. At the same time, the polarization of the TAE mode indicates that the perturbed parallel electric field is much smaller than electrostatic parallel electric field. In the current stage of HL-2A NBI heating experiment, low n TAE modes were not observed. However, the conditions to excite low n modes are obtained by simulation. Higher beam energy, for example $T_f = 80\,\mathrm{keV}$ and off-axis NBI heating, for example $\hat{\psi}_0 = 0.575$ are the necessary conditions to drive low n (e.g. $n = 1$) modes. The radial structures of low n TAE modes are usually more global than those of high n ones.

Acknowledgments

This work is supported by the National Natural Science Foundation of China grant Nos 11705050, 11775067, 11475057 and 11575158, the National Key R & D Program of China under Grant No. 2017YFE0300405, the National Magnetic Confinement Fusion Science Program under grant No. 2014GB124004 and the Scientific Research Key Foundation of the Education Department of Sichuan province with grant no.18ZA0471, Foundation of Sichuan University of Science and Engineering Grant No. 2016RCL21, Scientific Research Fund of the Sichuan Provincial Education Department Grant No. 17ZA0281 and US SciDAC ISEP Center.

ORCID iDs

Wenlu Zhang https://orcid.org/0000-0002-7136-2119
G.Z. Hao https://orcid.org/0000-0003-2310-6134
W. Chen https://orcid.org/0000-0002-9382-6295

References

[1] Cheng C.Z. and Chance M.S. 1986 *Phys. Fluids* **29** 3695
[2] Fu G.Y. *et al* 1989 *Phys. Fluids* B **1** 1949
[3] Cheng C.Z. 1991 *Phys. Fluids* B **3** 2463
[4] Nishimura Y. *et al* 2007 *Phys. Plasmas* **14** 042503
[5] Nishimura Y. 2009 *Phys. Plasmas* **16** 030702
[6] Mishchenko A. *et al* 2008 *Phys. Plasmas* **15** 112106
[7] Mishchenko A. *et al* 2009 *Phys. Plasmas* **16** 082105
[8] Lang J.Y. *et al* 2009 *Phys. Plasmas* **16** 102101
[9] Chen Y. *et al* 2010 *Phys. Plasmas* **17** 102101
[10] Berk H.L. *et al* 1992 *Phys. Fluids* B **4** 1806
[11] Wong K.L. *et al* 1992 *Phys. Fluids* B **4** 2122
[12] Ding X.T. *et al* 2013 *Nucl. Fusion* **53** 043015
[13] Chen W. *et al* 2014 *Europhys. Lett.* **107** 25001
[14] Zhu Y.B. *et al* 2010 *Nucl. Fusion* **50** 084024
[15] Ogawa K. *et al* 2010 *Nucl. Fusion* **50** 084005
[16] Matsunaga G. *et al* 2009 *Phys. Rev. Lett.* **103** 045001
[17] Lin Z. *et al* 1998 *Science* **281** 1835
[18] Zhang W. *et al* 2012 *Phys. Plasmas* **19** 022507
[19] Zhang C. *et al* 2013 *Phys. Plasmas* **20** 052501
[20] Wang Z. *et al* 2013 *Phys. Rev. Lett.* **111** 145003
[21] Cheng J. *et al* 2016 *Phys. Plasmas* **23** 052504
[22] Zhang H.S. *et al* 2010 *Phys. Plasmas* **17** 112505
[23] Liu F. *et al* 2010 *Phys. Plasmas* **17** 112318
[24] Deng W. *et al* 2012 *Nucl. Fusion* **52** 043006
[25] Deng W. *et al* 2010 *Phys. Plasmas* **17** 112504
[26] Zhang W. *et al* 2008 *Phys. Rev. Lett.* **101** 095001
[27] Zhang W. *et al* 2010 *Phys. Plasmas* **17** 055902
[28] Ishikawa M. *et al* 2007 *Nucl. Fusion* **47** 849
[29] Heidbrink W.W. *et al* 2007 *Phys. Rev. Lett.* **99** 245002
[30] Heidbrink W.W. *et al* 2008 *Nucl. Fusion* **48** 084001
[31] Zhang Y.P. *et al* 2015 *Nucl. Fusion* **55** 113024
[32] Hold I. *et al* 2009 *Phys. Plasmas* **16** 122307
[33] Lin Z. *et al* 2001 *Phys. Plasmas* **8** 1447
[34] Betti R. *et al* 1992 *Phys. Fluids* B **4** 1465
[35] Cheng C.Z. 1990 *Phys. Fluids* B **2** 1427
[36] Rosenbluth M.N. *et al* 1992 *Phys. Rev. Lett.* **68** 596
[37] Liu Y. *et al* 2008 *Phys. Plasmas* **15** 092505
[38] He H. *et al* 2011 *Nucl. Fusion* **51** 113012
[39] Yang S.X. *et al* 2018 *Nucl. Fusion* **58** 046016
[40] Liu Y. *et al* 2017 *Nucl. Fusion* **57** 114001